QTAIM Study on the Degenerate Cope Rearrangements of 1,5-Hexadiene and Semibullvalene

Eric C. Brown,*,† Richard F. W. Bader,*,‡ and Nick H. Werstiuk*,‡

Department of Chemistry, Loyola University, Chicago, Illinois, and Department of Chemistry, McMaster University, Hamilton, Ontario, Canada

Received: December 11, 2008; Revised Manuscript Received: January 22, 2009

Using the homotropylium cation (**1**) as an archetypal example of a homoaromatic molecule, we carried out a quantum theory of atoms-in-molecules (QTAIM) computational study—at DFT (density functional theory), CCSD (coupled cluster with singles and doubles), and CASSCF (complete active space self-consistent field) levels—on **1** and the degenerate Cope rearrangements of 1,5-hexadiene (**2**) and semibullvalene (**3**) including the evaluation of delocalization indexes and a visualization of atomic basins. This study yielded new insights into the factors determining the reaction barriers and the bonding of the ground and transitions states of **2** and **3**. Contrary to conclusions reached in earlier studies, we found that the transition state for the degenerate rearrangement of **2** is not aromatic and that the driving force for the very facile Cope rearrangement of semibullvalene is caused by the stabilization of individual atoms as well as electronic delocalization, not by the release of strain in the three-membered ring.

Introduction

The homotropylium cation (**1**) (Scheme 1) considered as the archetypal example of a species exhibiting homoaromaticity has been the subject of countless computational and experimental studies.[1] The degenerate Cope rearrangements of 1,5-hexadiene (**2**) (Scheme 1)—its transition state is considered to be aromatic—and its equivalent in fluxional molecules like semibullvalene (**3**) (Scheme 1), barbaralane, and its heteroatom analogues have also captured the interest of experimentalists and theoreticians for decades because of the possibility of these neutral molecules and their transition states exhibiting homoaromatic behavior. It is known that, unlike **2**, semibullvalene exhibits a very low degenerate-rearrangement barrier. Excellent accounts of the field have been documented in many papers and reviews based on experimental and computational studies.[2−9] It has been proposed that this be accounted for not on the basis of (bis)homoaromatic stabilization of the C_{2v} transition state but rather predominately on the relief of strain and the fact that compounds of this type are already fixed in the appropriate boat conformation by the bridge between C1 and C5.[6,7] In an effort to lower the barrier further and obtain biradical or biradicaloid ground states, researchers have studied a variety of substituted semibulvalenes experimentally and computationally. For the degenerate Cope rearrangement of **2**, the results of the most recent high-level computational study led the conclusion that the wave function of the transition state (**2-TS**) is best described as being closed-shell without significant biradicaloid character.[10]

We demonstrate herein that the competing rationales for the lower barrier in semibullvalene—relief of strain in the closed form **3** or (bis)homoaromatic stabilization in its transition state (**3-TS**)—are readily distinguished from one another using the quantum theory of atoms-in-molecules (QTAIM).[11] Winstein's definition of homoaromaticity[12] proposes a mode of electron delocalization that should have measurable consequences on the distribution of the electron density and the energy, proffering an example of the ability of QTAIM to transcribe the electronic arguments of an orbital model into physical properties that characterize a charge distribution.[11] The chemical concepts of "strain energy" and "resonance stabilization" necessary for a discussion of this problem find physical expression in the QTAIM definition of the energy of an atom in a molecule.

A recent paper[13] demonstrated that QTAIM is derivable from the Schrödinger equation using an appeal to experiment to establish the "zero-flux" boundary condition. It is the zero-flux boundary condition that defines an atom and its properties. The presence of a bond path is but a useful way of depicting which

SCHEME 1

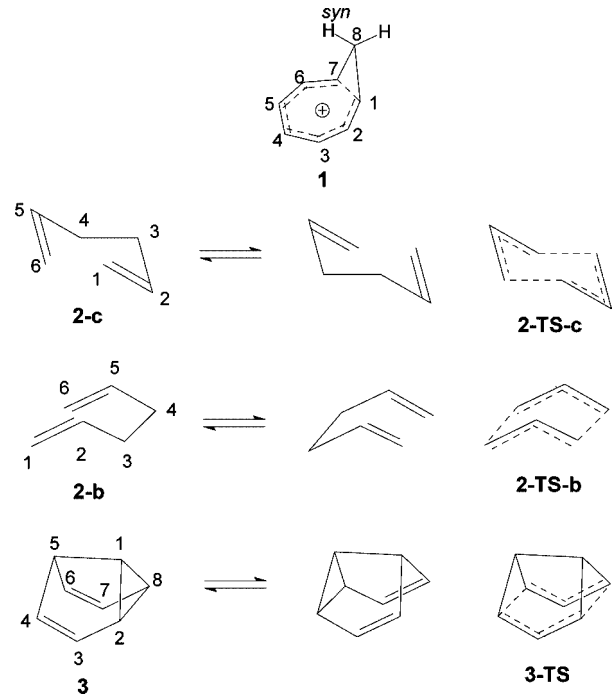

* Corresponding authors.
† Loyola University.
‡ McMaster University.

10.1021/jp8109385 CCC: $40.75
Published on Web 03/10/2009

TABLE 1: Selected Calculated and Experimental Interatomic Distances (angstroms)

level[a]	C1−C2	C1−C8	C2−C3	C7−C8	C3−C4	C5−C6	C6−C7	C1−C7	C2−C8	C4−C6
1(B3PW91)	1.382	1.480	1.392	*b*	1.395	*b*	*b*	2.016		
1(PBE1PBE)	1.386	1.476	1.388	*b*	1.395	*b*	*b*	1.941		
1(CCSD(full)/6-31+G(d,p))	1.385	1.485	1.404	*b*	1.403	*b*	*b*	2.066		
2-C_2-c(B3PW91)	1.327				1.539	1.327				
2-C_1-b(B3PW91)	1.327				1.540	1.327				
3(B3PW91)	1.495	*b*	1.466	*b*	1.339		*b*		1.601	2.335
3(PBE1PBE)	1.495		1.464		1.338				1.595	2.327
3(CCSD(full)/6-31+G(d,p))	1.501		1.483		1.347				1.575	2.378
3(CASSCF(6,6))	1.489		1.487		1.340				1.550	2.405
3(exptl)[b,c]	**1.530**		**1.531**		1.350				1.600	2.261

[a] Calculations at the 6-311+G(2d,p) level unless stated otherwise. [b] Interatomic distances related by symmetry not included. [c] See ref 30.

TABLE 2: Selected Calculated Interatomic Distances (angstroms) of Transition States and IRC Points

compd	C1−C2	C2−C3	C3−C4	C4−C5	C2−C8	C4−C6
2-TS-C_{2h} (B3PW91)[a]	1.403	*b*	1.914	*b*		
2-TS-C_{2h} (PBE1PBE)	1.404	*b*	1.881	*b*		
2-TS-C_{2v} (B3PW91)	1.387	*b*	2.171	*b*		
2-TS-C_{2v}(PBE1PBE)	1.387	*b*	2.126	*b*		
3-TS-C_{2v} (B3PW91)	1.494	1.384	*b*	1.494	2.062	*b*
3-IRC-PT 21(B3PW91)	1.488	1.452	1.344	1.514	1.689	2.269
3-IRC-PT 22(B3PW91)	1.489	1.455	1.344	1.515	1.674	2.277
3-TS-C_{2v} (PBE1PBE)	1.492	1.384	*b*	1.492	2.036	*b*
3-TS-C_{2v} (CCSD(full)/6-31+Gd,p))	1.499	1.392	*b*	1.499	2.078	*b*
3-TS-C_{2v} (CASSCF(6,6)	1.501	1.386	*b*	1.501	2.289	*b*

[a] Calculations at the 6-311+G(2d,p) level unless stated otherwise. [b] Interatomic distances related by symmetry not included.

TABLE 3: Thermochemical Data of 2 and Transition States at B3PW91/6-311+G(2d,p)

	2-C_2-c	**2-TS-C_{2h}**	barrier (kcal mol^{-1})[a]	**2-C_1-b**	**2-TS-C_{2v}**	barrier (kcal mol^{-1})[a]
E_{elec}[b]	−234.590827	−234.538773 (−547.3)[c]	32.66	−234.591418	−234.523766 (−542.2)[c]	42.45
E_0[d]	−234.449495	−234.397703	32.50	−234.449859	−234.384004	41.32
E_{298}[e]	−234.442136	−234.391793	31.59	−234.442589	−234.377635	40.76
H_{298}[f]	−234.441192	−234.390849	31.59	−234.441645	−234.376690	40.76

[a] The $\Delta E^{\ddagger}_{elec}$, $\Delta E^{\ddagger}_{0}$, $\Delta E^{\ddagger}_{298}$, and $\Delta H^{\ddagger}_{298}$ values. [b] E_{elec} is the uncorrected total energy in hartrees. [c] The imaginary frequency (cm^{-1}). [d] $E_0 = E_{elec}$ + ZPE. [e] $E = E_0 + E_{vib} + E_{rot} + E_{trans}$. [f] $H = E + RT$.

atoms share an interatomic surface, one that recovers the manner in which the same information is conveyed by the structures that evolved from experimental chemistry. Thus, the properties associated with an atom or a bond path follow directly from Schrödinger's equation. Because it is the presence of an interatomic surface that is the necessary condition for two atoms to be bonded to one another, QTAIM employs the symbol A|B to denote bonding between A and B rather than A−B.

As far as we are aware no QTAIM[11] or QTAIM-DI-VISAB[14−18] studies have been reported on **2** or fluxional molecules such as **3** and its substituted analogues which undergo the equivalent of the Cope rearrangement. This paper reports the results of QTAIM studies on the rearrangements of **2** and **3** as well the molecular structure of the homotropylium cation (**1**), considered to be the archetypal example of a homoaromatic species.

Computational Methods

Density functional theory (DFT) ((U)B3PW91 and (UP)BE1PBE) and calculations were carried out with Gaussian 03 (G03)[19] at the 6-311+G(2d,p) level on **1**, **2**, **3**, and transition states (TSs). Unrestricted calculations carried out with GUESS = MIX converged to the RHF wave function with $\langle S^2 \rangle = 0$. Vibrational analyses were performed for all structures in order to confirm minima and transition states and provide the thermochemical data necessary to evaluate reaction barriers. Our previous experiences with DFT calculations on carbocations[16,18,20] clearly showed that the B3PW91 and PBEPBE1 hybrid functionals were superior to B3LYP—to this point the DFT method of choice for studying bishomoaromaticity in semibullvalenes[6−9,21]—in computing the geometries of delocalized alleged nonclassical species. Consequently, we used the B3PW91 and PBE1PBE functionals but focus on the B3PW91 results in this paper. CCSD(full) calculations on **1** and **3** were done at the 6-31+G(d,p) level to reduce the long CPU times that would be required to carry out the studies at 6-311+G(2d,p) basis. Calculations were also carried out on **3** and **3-TS** at the CASSCF(6,6)/6-311+G(2d,p) level with GUESS = PERMUTE, the rationale being that **3-TS** could be viewed as two weakly interacting allylic radicals. GaussView 3.0[22] was used to fix C_S, C_2, and C_{2v}, C_{2h} symmetries where necessary and to confirm that the three highest occupied CASSCF molecular orbitals (MOs) of **3** and **3-TS** were π-type. Selected calculated and experimental internuclear distances of **1**, **2**, and **3** are collected in Table 1, and calculated internuclear distances of TSs of **2**, and **3** are given in Table 2. An intrinsic reaction coordinate (IRC) calculation was carried out on **3-TS-C_{2v}** using the G03 default step-size to ascertain at what point the C2|C8 bond path was cleaved. Total energies and thermochemical data are collected in Tables 3−5 and Tables 1S and 2S as Supporting Information. Although we computed $\Delta E^{\ddagger}_{elec}$, $\Delta E^{\ddagger}_{0}$, $\Delta E^{\ddagger}_{298}$, and $\Delta H^{\ddagger}_{298}$ for the rearrangements, only $\Delta E^{\ddagger}_{elec}$ and $\Delta H^{\ddagger}_{298}$ are included in the discussion. The results of calculations on ethane, ethene, and ethyne are not reported.

TABLE 4: Total Energies and Thermochemical Data of 3-C_S and 3-TS-C_{2v} at (U)B3PW91/6-311+G(2d,p)

	3-C_S	3-TS-C_{2v}	barrier (kcal mol^{-1})[a]
E_{elec}[b]	−309.548464	−309.539578 (−267.7)[c]	5.69
E_0[d]	−309.414470	−309.407281	4.51
E_{298}[e]	−309.409106	−309.401973	4.47
H_{298}[f]	−309.408161	−309.401029	4.47

[a] The $\Delta E^{\ddagger}_{elec}$, $\Delta E^{\ddagger}_0$, $\Delta E^{\ddagger}_{298}$, and $\Delta H^{\ddagger}_{298}$ values. [b] E_{elec} is the uncorrected total energy in hartrees. [c] The imaginary frequency (cm^{-1}). [d] $E_0 = E_{elec} + ZPE$. [e] $E = E_0 + E_{vib} + E_{rot} + E_{trans}$. [f] $H = E + RT$.

Results of QTAIM analyses carried out with AIM 2000[23] are collected in Table 3S (Supporting Information). Delocalization indexes (DIs)[24] for selected atom pairs were obtained with LI-DICALC[25−27] and are listed in Tables 4S and 5S (Supporting Information). Displays of molecular graphs (Figures 1−6 and Supporting Information Figure 1S) and atomic basins were obtained with AIM 2000. Atomic basins were obtained at a contour value of 0.005 au—this includes greater than 95% of the electrons—using a mesh grid size of 0.125 and plotted with a sphere size of 0.15. AIMALL97[28] was used for QTAIM integrations to obtain atom energies (Supporting Information Tables 6S−8S) and atomic overlap matrices required for calculation of DIs. Atomic basins are displayed in Figure 1 and Figures 3−5.

ChemCraft[29] was used to animate the normal modes obtained with G03 frequency calculations. The 175 cm^{-1} mode of **1**, the one that appears to bring C1 and C7 within a distance where a bond path might be formed, was selected for a detailed "displacement" analysis with ChemCraft. In order to "generate" a bond path between C1|C7 it was necessary to scale the G03 displacement coordinates by 0.65 and freeze the nuclear motions at a point where the C1|C7 distance was 1.612 Å. A Cartesian-coordinate file was written at this point and a single-point calculation was carried out with SCF = TIGHT to obtain a wave function. The uncorrected electronic energy E_{elec} of the 1.612 Å geometry was −309.905226 hartree, and ΔE_{elec} relative to the equilibrium geometry was 5.90 kcal mol^{-1}. A "displacement" analysis was also carried out on the 474 cm^{-1} mode of **3**.

Results and Discussion

Molecular Geometries. ***Starting Compounds and Transition States.*** Selected computational and experimental internuclear distances are collected in Table 1. In the case of the equilibrium geometry of **1**, the crucial C1−C7 distances fall in the range of 2 Å; 2.016, 1.941, 2.066 Å at B3PW91, PBE1PBE, and CCSD, respectively. The H7$_{syn}$−C4 distances are 2.746, 2.748, and 2.695 Å at B3PW91, PBE1PBE, and CCSD, respectively. For **2**, conformations **2-C_2-c** and **2-C_1-b** whose molecular graphs are displayed as Figure 1S, parts a and b (Supporting Information), respectively, were used to calculate the barriers for the degenerate rearrangement of **2**. There are a number of differences between the computational and experimental data for **3** that warrant discussion. On the basis of the calculations at the B3PW91, PBE1PBE, CCSD, and CASSCF levels, the C1−C2 and C2−C3 distances obtained with gas-phase electron diffraction[30] for **3** appear to be too long in keeping with the conclusions reached by Christoph and Beno.[31] Nevertheless, there is good agreement between the calculated and experimental values for C3−C4, C2−C8, and C4−C6 at B3PW91—the B3PW91 molecular graph of **3** is displayed as Figure 3a—and PBE1PBE (molecular graph not shown) yielding better values for the longest cyclopropyl C−C (C2−C8) bond than the other levels of theory; CCSD, and CASSCF yield a C2−C8 internuclear distance significantly smaller than the experimental. In fact, the CASSCF (Table 1) distances for C2−C8 and C4−C6 deviate the most from the experimental values.

In the case of the Cope rearrangement, the boat TS **2-TS-C_{2v}** exhibits significantly longer C3−C4 and C1−C6 bonds (2.171 Å, B3PW91; 2.126 Å, PBE1PBE) than the chair TS **2-TS-C_{2h}** (1.914 Å, B3PW91; 1.881 Å, PBE1PBE). That the boat TS **2-TS-C_{2v}** is a little looser—the partial single bonds are weaker—than **2-TS-C_{2h}** is in keeping with the fact that computed barriers differ by ∼10 kcal mol^{-1}.

In the case of the rearrangement of **3**, the C2−C8 and C4−C6 distances of **3-TS-C_{2v}** are slightly larger than 2 Å; 2.062, 2.036, and 2.078 Å at B3PW91, PEB1PBE, and CCSD, respectively. The CASSCF distance of 2.289 Å deviates significantly from the B3PW91, PEB1PBE, and CCSD values.

Reaction Barriers. To further validate the use of the B3PW91 hybrid functional, we computed the barriers for selected degenerate rearrangements and compared the results with experimental values. Because of the conformational mobility of **2** there is an infinite number of conformations possible for the starting geometry, so a computed barrier depends on the starting conformation. The thermodynamic parameters collected in Table 3 (B3PW91) and Supporting Information Table 1S (PBE1PBE) are based on using conformers **2-C_2-c** (Supporting Information Figure 1Sa) and **2-C_2-b** (Supporting Information Figure 1Sb) that were obtained by optimizing the end points obtained from reverse-direction IRC calculations. From this point on, only the B3PW91 results will be discussed. The values of $\Delta E^{\ddagger}_0$ and $\Delta H^{\ddagger}_{298}$ based on **2-C_2-c** and its chair transition state **2-TS-C_{2h}** (Figure 3a are 32.50 and 31.59 kcal mol^{-1} at B3PW91 (Table 3). The computed $\Delta H^{\ddagger}_{298}$ value is in excellent agreement with the experimental value of $\Delta H^{\ddagger}_{500}$ (33.5 ± 0.5 kcal mol^{-1}).[32] Between **2-C_2-b** and its boat transition state **2-TS-C_{2v}**, the $\Delta E^{\ddagger}_0$ and $\Delta H^{\ddagger}$ values (41.32 and 40.76 kcal mol^{-1}) are considerably higher than for the chair conformation at B3PW91, in keeping with the results of a previous computational study.[33] In the case of **3** the B3PW91 (Table 4) values for $\Delta E^{\ddagger}_0$ and $\Delta H^{\ddagger}_{298}$ are 4.51 and 4.47 kcal mol^{-1}, nicely in accord with the best experimental value of 5.2 kcal mol^{-1} for $\Delta H^{\ddagger}$.[34,35] Because we planned to use the 6-31+G(d,p) basis set for the calculations at the CCSD level we carried out calculations on **3** with this basis set as well. Although $\Delta E^{\ddagger}_0$ and $\Delta H^{\ddagger}_{298}$ are marginally higher (5.00 and 4.97 kcal mol^{-1}) at this B3PW91 lower level, the results established that the 6-31+G(d,p) basis set would be acceptable for CCSD calculations on **3**. CCSD-(full)/6-31+G(d,p) results on **3** and **3-TS-C_{2v}** are collected in Table 5; at this level, $\Delta E^{\ddagger}_{elec}$ and $\Delta E^{\ddagger}_0$ values are 12.29 and 11.38 kcal mol^{-1}, roughly twice as large as the experimental value for $\Delta H^{\ddagger}_{298}$. Also included in this table are CASSCF(6,6)/6-311+G(2d,p) data. At CASSCF(6,6)/6-311+G(2d,p) **3-TS-C_{2v}** is lower in energy (−2.38 kcal mol^{-1}) than **3**, out of line with the experimental result.

Homoaromaticity. The transcription of Winstein's homoaromatic model into the properties of the charge distribution is documented in the literature,[36] most recently in an extensive review by Cremer et al.[37] The original topological criteria for the presence of homoconjugative bonding have been extended to include a physical measure of electron delocalization in terms of the exchange density[24] and a determination of the energetic stabilization derived from the delocalization of the density. The

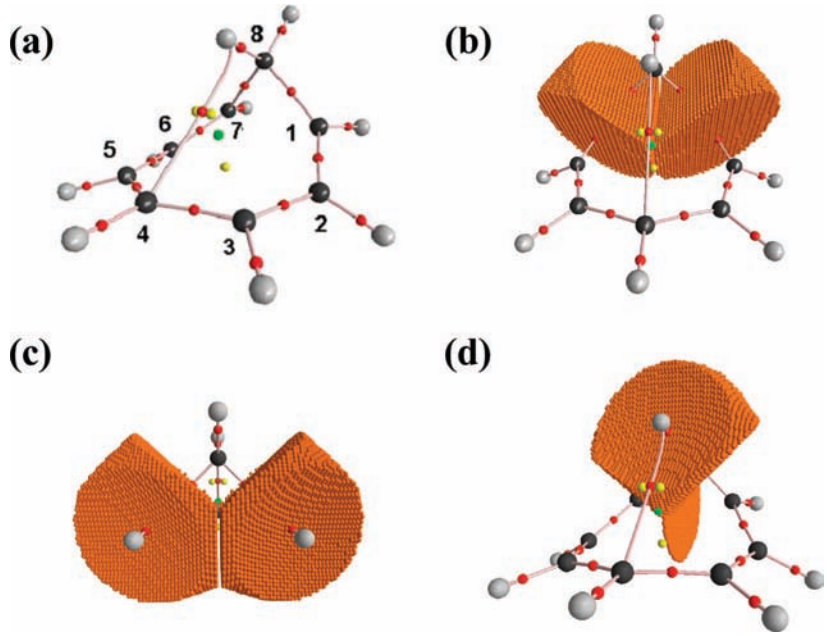

Figure 1. (a) Molecular graph of **1** (carbon and hydrogen atoms shown as black and gray spheres, respectively; red spheres are bond cps, yellow spheres are ring cps, and green spheres are cage cps); (b) C1 and C7 basins of **1**; (c) rear view of C1 and C7 basins of **1**; (d) C8 basin of **1**.

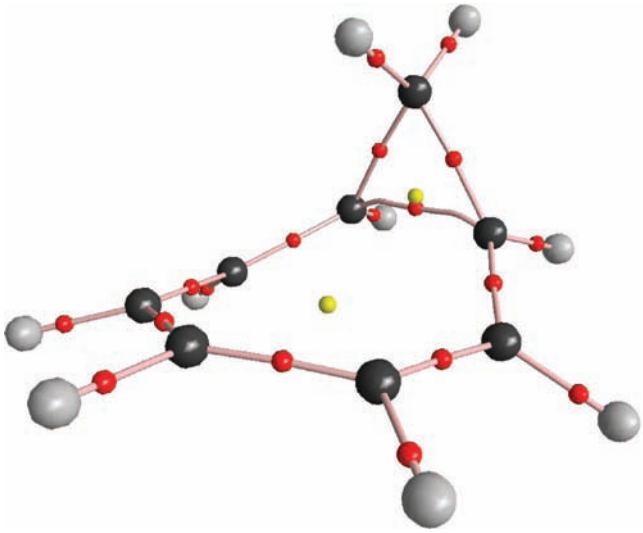

Figure 2. Molecular graph of the 1.612 Å geometry of **1**. Note the proximity of the bond and ring cps of the 3-MR indicating its potential instability.

physical criteria for homoaromatic conjugation are first reviewed and illustrated through their application to the homotropylium cation.

Bond Order. There are two physical measures of bond order n. One is determined by fitting the value of ρ_b, the value of the density at a bond critical point (cp), to an empirical two-parameter expression[11] that yields orders of 1.0, 1.6, 2.0, and 3.0 for the C|C bond paths in ethane, benzene, ethene, and ethyne, respectively ($n = \exp[A(\rho_b - B)]$ where $\rho_b = 0.2394$, its value for ethane and $B = 6.070$ for the B3PW91/6-311++G(2d,p), calculations. Values of $\rho(r)$ at bond cps can be used to qualitatively assess relative covalent bond strengths. The second is determined by the pair density and expressed in terms of the delocalization index, DI(A|B),[24−27] that determines the extent of exchange of electrons between two atomic basins A and B.

The DI for two bonded carbon atoms yields the number of "shared electron pairs" with values of 1.0, 1.4, 1.9, and 2.9 for the above set of molecules, in qualitative agreement with the Lewis model. DI(A|B) is an important parameter especially in the discussion of homoaromaticity because the possibility exists to have a significant degree of delocalization/sharing of electrons without having a bond path linking the atomic basins. This turns out to be an important physical signature of homoaromatic character.

Bond Ellipticity. The electron density of a bond that in an orbital model possesses "π" character is elliptically disposed about the bond path (bp). The electron density is preferentially accumulated in a plane that in ethene is perpendicular to the plane of the nuclei, the plane determined by the major axis of the ellipse. The extent of this accumulation is determined by the ellipticity defined as $\varepsilon = \lambda_1/\lambda_2 - 1$ where λ_1 and λ_2 are the negative eigenvalues of the Hessian of the electron density with respect to position.[11] That is, the curvatures of the density at the bond cp perpendicular to the bond path, with $|\lambda_1| > |\lambda_2|$, λ_2 being the curvature along the major axis of the ellipse, that is, the direction of the "soft" curvature. The ellipticities of the C−C bonds in ethane, benzene, and ethylene are 0.0, 0.18, and 0.30, respectively. The ellipticity has the property of determining the presence of a π-like component to the density, even in situations where the bond order is less than unity.

Obviously, this parameter is available only in cases where a bond path connects two atoms.

Aromaticity and Homoaromaticity in Terms of Bond Descriptors and Atomic Energies. The concept of homoaromaticity introduced by Winstein in 1959[38] is used to rationalize the stability and reactivity of an unsaturated segment linked to a cyclopropane moiety by invoking its electronic similarity to an aromatic system. Aromaticity in a cyclic unsaturated system is defined here as one in which there is a delocalization of the electrons over a conjugated ring of carbon atoms: bond orders and delocalization indices in excess of unity and nonvanishing bond ellipticities whose major axes are parallel to the ring axis (that is, perpendicular to the plane of the ring). These descriptors of aromaticity when applied to the planar tropylium cation $C_7H_7^+$, describe a ribbon-like delocalization of "π" density around the carbons of the ring. The ellipticities are 0.13 with

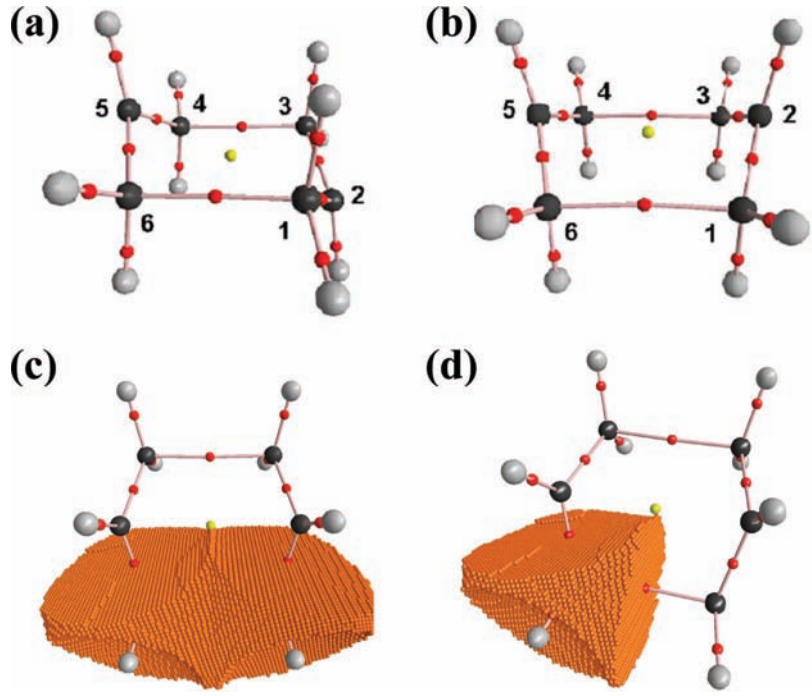

Figure 3. (a) Molecular graph of **2-TS-C_{2h}**; (b) molecular graph of **2-TS-C_{2v}**; (c) C1 and C6 basins of **2-TS-C_{2v}**; (d) C1 basin of **2-TS-C_{2v}**.

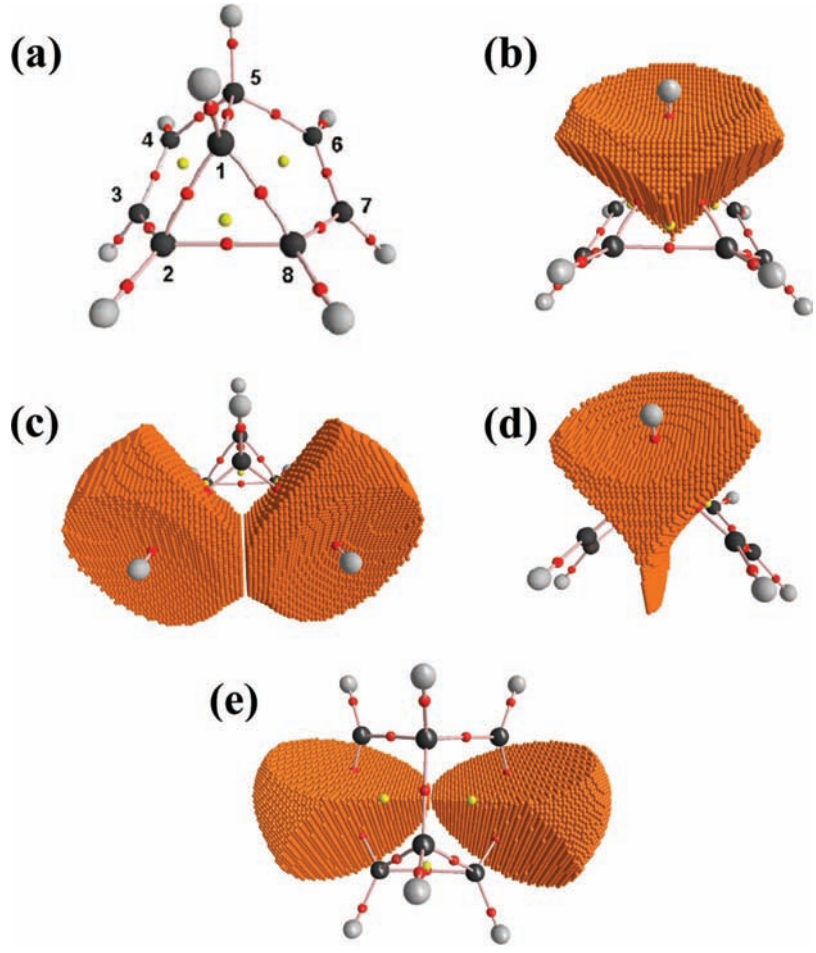

Figure 4. (a) Molecular graph of **3**, (b) C1 basin of **3**, (c) C4 and C6 basins, (d) C5 basin, and (e) C3 and C7 basins.

their major axes parallel with the ring axis; bond orders are 1.6, and DIs are 1.4. These values compared well with the corresponding values in benzene of 0.18, 1.6, and 1.4 at the B3PW91/6-311+G(2d,p) level.

Electron Delocalization in Cyclopropane. The chemistry of cyclopropane emulates that of an unsaturated system. This is accounted for in MO theory by Walsh orbitals which ascribe π character to orbitals lying in the plane of the ring.[39,40] QTAIM

TABLE 5: Total Energies and Thermochemical Data of 3 and Transition States at (U)CCSD(full)/6-31+G(d,p) and CASSCF(6,6)/6-311+G(2d,p)

	(U)CCSD(full)/6-31+G(d,p)			CASSCF(6,6)/6-311+G(2d,p)		
	3-C_S	**3-TS-C_{2v}**	barrier (kcal mol^{-1})[a]	**3-C_S**	**3-TS-C_{2v}**	ΔE_{elec} (kcal mol^{-1})
E_{elec}	−308.708970[b]	−308.689385[b]	12.29	−307.644153	−307.647927	−2.38[a]
E_0[c]	308.573334 (ZPE = 0.135626)[d]	308.555200 (ZPE = 0.134185)[d] (−82.1)[e]	11.38			

[a] The $\Delta E^{\ddagger}_{elec}$, and $\Delta E^{\ddagger}_0$, values. [b] E_{elec} is the uncorrected CCSD total energy in hartrees. [c] $E_0 = E_{elec} + ZPE$. [d] ZPVE in hartrees obtained at MP2(full)/6-31+G(d,p). [e] The imaginary frequency (cm^{-1}).

gives physical substance to this model by determining that the C|C bond paths exhibit significant ellipticities whose major axes lie in the ring surface. This is a topological consequence of the proximity of the ring and bond critical points unique to a three-membered ring (3-MR). Because of the accumulation of density within the ring's interior, the value of the density at the ring cp approaches its value at the bond cps for the C|C bond paths of the ring, the value of the latter exceeding that of the former by only 0.05 au in cyclopropane. The result is a delocalization of the density over the surface of the ring with the major axis of the C|C bond cps lying in the surface of the ring. Thus, as postulated by Winstein,[12] cyclopropane may enter into conjugation with an unsaturated system when the ring surface is properly aligned, giving rise to homoconjugated and homoaromatic interactions. An example of the former is cyclopropyl carbinyl cation $C_4H_7^+$, wherein the ring surface is conjugated with an empty p orbital on a CH_2 group. The documented lability of this system is quantified in terms of its structure diagram describing the intermediates involved with the scrambling of the methylene groups.[41] An example of the latter case, as discussed below, is a structure of the homotropylium cation $C_8H_9^+$ obtained when a CH_2 group is inserted into $C_7H_7^+$.

Determining Homoaromatic Stabilization and Strain Energies. The ability to define the energy of an atom in a molecule enables one to determine two important quantities for a discussion of homoaromaticity: aromatic stabilization and strain energy. To quote Winstein: "Just as for aromaticity, one criterion for homoaromaticity is increased stability or delocalization energy of a substrate because of cyclic electron delocalization".[12] QTAIM energies for carbon atoms are in line with the hybridization model, an increasing "s over p character" leading to an increase in stabilization and electronegativity, as reflected in an increasing withdrawal of electrons from a bonded H. The carbon atom energies in ethane, ethene, and ethyne yield a near linear relationship with respect to their atomic populations at B3PW91/6-311+G(2d,p) with a regression coefficient of 0.996. The resulting "linear charge/energy relationship" displayed in Supporting Information Figure 2S enables one to determine the extent to which a carbon atom is stabilized in a system with electron delocalization. A carbon atom in benzene with a population intermediate between that in ethane and ethene, for example, is more stable than that predicted by the linear charge/energy relationship by 17 kcal mol^{-1}. It is also 10.0 kcal mol^{-1} more stable than the corresponding atom in the |CH group of *cis*-1,3-butadiene, as would be expected on the basis of the resonance model. However, the H atom in butadiene possesses a slightly greater electron population and is consequently 3.5 kcal mol^{-1} more stable than H in benzene, making the |CH group 6.5 kcal/mol more stable in benzene than in butadiene. Thus, the increased stability of a |CH group in benzene over the same nonconjugated group of *cis*-butadiene as determined by QTAIM, yields a "resonance" energy of $6 \times 6.5 = 39$ kcal mol^{-1}. On the basis of the |CH group of cyclohexhene, the predicted "resonance" energy is 41 kcal mol^{-1}. The generally accepted value for the resonance energy of benzene is 37−41 kcal mol^{-1}, the higher values being obtained from heats of combustion.[42] These results clearly validate analyses based on atom energies.

A carbon atom in tropylium, which bears a net positive charge of 0.017e, is correspondingly stabilized by 22 kcal mol^{-1} at B3PW91/6-311+G(2d,p).

As noted above, cyclopropane behaves in some respects, as an unsaturated system. Because of the angle strain in a 3-MR and the concomitant increase in the p character of the C−C bonds, the s character of the bonds to H is increased and the carbon atoms approach ethylenic carbons in electronegativity.[43] Coulson and Moffitt emphasize this point in their classic study of strain in cyclopropane by noting that the bond lengths and bond angles of the methylene group in cyclopropane resemble those for ethylene.[44] This has the effect of increasing the stability of a cyclopropane carbon relative to its unstrained analogue, and ring strain is not a result of a destabilization of the carbon atoms but of their bonded hydrogens following the loss of electron density to the carbons. Thus, the atomic populations and energies of the methylene group in cyclopropane are similar with the CH_2 group of ethene being 3 kcal mol^{-1} more stable than in ethene. *The transfer of density from the H atoms to C causes the energies of the two H atoms to increase more than the energy of the C atom decreases, and the CH_2 group of cyclopropane is less stable than the standard transferable methylene group of saturated hydrocarbons by 9.2 kcal mol^{-1}.* It is important to note that this value equals one-third of the so-called strain energy of cyclopropane estimated to be 27.5 kcal mol^{-1} from thermochemical measurements.[45] This transfer of density from H to C decreases with the size of the ring and vanishes for cyclohexane, which is consequently predicted to have zero strain energy, in agreement with experiment. One should note that this definition of strain energy is not determined by symmetry—that the energy of an *n*-cyclic hydrocarbon is $1/n$ that of the total. The strain energy is determined by comparing $1/n$ of the cyclic energy with the energy of the standard methylene group defined by the linear regression analysis of the energies of the linear hydrocarbons, the quantity $E°(CH_2)$. This energy is determined theoretically by integration of the electronic kinetic energy density over a region of space bounded by the two C|C zero-flux surfaces bounding the $|CH_2|$ group, using the virial theorem of an open system. The finding that this energy is given by precisely the slope $E°(CH_2)$ (to within 0.2 kcal/mol) assigned to the methylenic energy in a linear regression analysis of the linear hydrocarbon energies is striking proof of the physical relevance of the zero-flux surface and of the energies defined by QTAIM.

The hybridization model is simple and powerful; s electrons are bound more tightly than p electrons, and hybridization is determined primarily by bond angles. This model and its recovery in the atomic properties of QTAIM is of particular importance in the discussion of the role of "strain" in the chemistry of semibullvalene.

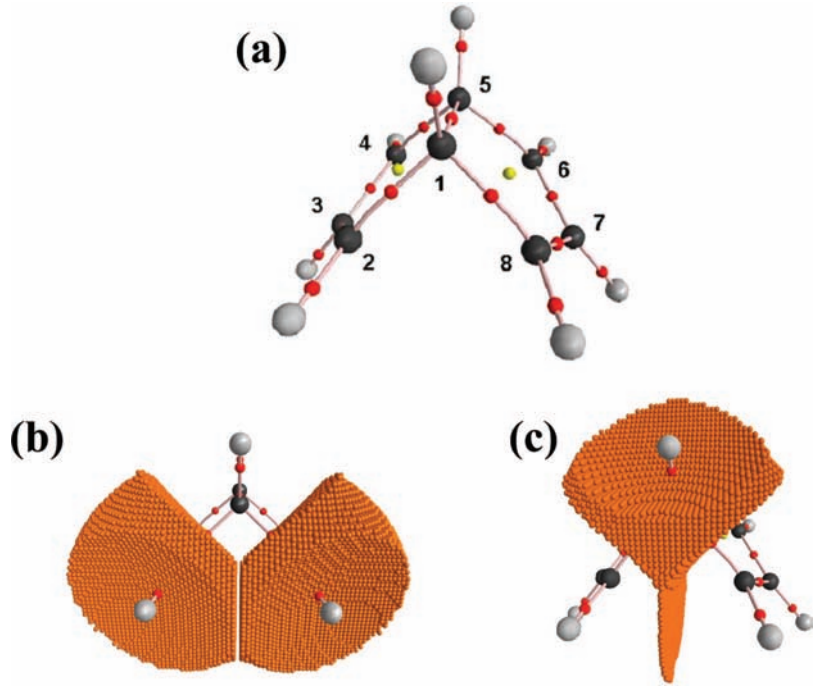

Figure 5. (a) Molecular graph of **3-TS-C_{2v}**, (b) C2 and C8 basins of **3-TS-C_{2v}**, and (c) C2 basin of **3-TS-C_{2v}**.

Homoaromaticity in the Homotropylium Cation. At its equilibrium geometry **1** does not exhibit a C1|C7 path, as determined by Cremer et al. at MP2/6-31G(d)[46] and all levels of theory used here. The molecular graph of **1** obtained in this work at B3PW91/6-311+G(2d,p) level is displayed as Figure 1a. This is contrary to an initial report employing a low level of theory that underestimated the C−C separations, particularly that of C1−C7.[36] It is interesting to note that we also find a bond path between the syn H at C8 and C4. Figure 1, parts b and c, display two orientations—front and back—of the C1 and C7 atomic basins. Figure 1d shows the C8 basin that exhibits a "wedge" of density between C1 and C7 thereby precluding bond path formation between these atoms. Nevertheless, homotropylium cation serves as the ideal prototype for relating Winstein's experimental criteria for homoaromaticity to the properties of the electron density. This is a consequence of perhaps the most important of the properties associated with a molecule exhibiting homoaromatic behavior: its facility to structural change. To establish whether a bond path materializes due to nuclear motions, a displacement analysis was executed on the low-frequency 175 cm^{-1} mode of **1** because this mode was found to decrease the C1−C7 distance relative to its value in the equilibrium geometry. In the manner detailed in the Computational Methods, freezing the nuclear motions for this mode so as to reduce the C1−C7 separation to 1.612 Å resulted in the linking of C1 to C7 by a bond path with an energy increase of 5.90 kcal mol^{-1} over the equilibrium geometry. The molecular graph of the 1.612 Å species is displayed as Figure 2. The syn H|C4 bond path is lost in going from the equilibrium geometry to the 1.612 Å one. Given that the zero-point energy (ZPE) of the 175 cm^{-1} mode is only 0.25 kcal mol^{-1}, homotropylium does not exhibit a C1|C7 bond path at 0 K. The average geometry of **1**—the C1−C7 distance (1.997 Å) is marginally smaller than the C1−C7 distance of the equilibrium structure—computed with G03 using the keywords FREQ = ANHARM and also does not exhibit a C1|C7 bond path at 0 K.

An important conclusion to be made from the discussion that follows is that it is not necessary for a system to exhibit a bond path in its equilibrium geometry to exhibit homoaromatic behavior. What is necessary is that the molecule possesses an internuclear region or regions wherein the density is characterized by low curvatures resulting from electron delocalization, a condition that enables facile nuclear motions. It is remarkable how well a model of electron delocalization based on experimental solvolysis rates maps onto a particular set of properties of a molecular charge distribution. Homoaromaticity, for example, is shown to be a direct consequence of the unique delocalization of the electron density found over the surface of a 3-MR or pseudo-three-membered ring (PS-3-MR).

The C1|C7 bond path "closing" the 3-MR in the 1.612 Å structure of **1** (Figure 2) possesses a bond order equal to 0.70, a delocalization index of 0.70—as opposed to a DI of 0.35 for the equilibrium geometry—and a pronounced ellipticity equal to 5.9. The properties of the remaining C−C bond paths of the 7-MR emulate those found for the homotropylium cation. The major axes of the ellipticities of all C|C bond paths of the 7-MR closely parallel the axis of the 7-MR thus indicating the presence of a ribbon-like delocalization of "π" density around the carbons of the ring. The major axis of the homoaromatic bond path is parallel to the ring axis of the 7-MR and perpendicular to the ring axis of the 3-MR, the relative alignments required for maximizing the extent of aromatic conjugation between the 3- and 7-MRs as envisaged by Winstein.

The carbon atoms of the 7-MR are all stabilized with respect to the linear energy relationship, with an average value of 18 kcal mol^{-1} representing a slight increase over the value in the equilibrium structure. The formation of the C1|C7 bond path, however, increases the stabilization of C1 and C2 by 6 kcal mol^{-1} each over their values in the open structure. Thus, homotropylium exhibits all of the hallmarks of homoaromaticity, as judged by the values of the bond descriptors resulting from the presence of a significant delocalization of π-like density over the carbons of the 7-MR and by the stabilization of the ring atoms.

Homoaromaticity and Singularities in the Density. Although no C1|C7 bond path is present in the equilibrium geometry of **1**, there is a significant delocalization of electrons between their

atomic basins, with DI(C1|C7) = 0.35. At CCSD(full)/6-31+G(d,p) where the C1−C7 distance is 2.066 there is no C1|C7 bond path and the DI(C1|C7) = 0.24. Relatively large nonbonded DIs denote the presence of a flat density distribution between the atomic basins. A zero curvature in the density is the requirement for the formation of a singularity in the density, giving rise to a bond path and the associated ring structure. The individual curvatures in the density at the midpoint between C1 and C7 in the equilibrium structure of **1**, for example, are small with $\nabla^2\rho = -0.04$ au and with a value for the density equal to 0.10 au. This is equivalent to a bond order of 0.43 and is of the order required for the formation of a bond path.

The section on the Electron Delocalization in Cyclopropane described how the delocalization of the density over the surface of a 3-MR was a consequence of the proximity of the ring and bond critical points, the small differential in their values resulting from the accumulation of density within the ring's interior. Thus, the value of the density at a bond cp in cyclopropane exceeds the value at the ring cp by only 0.05 au. The result is a delocalization of the density over the surface of the ring leading to a softening of the in-plane curvature of each bond cp and to large ellipticities, the ellipticities of ring bonds, equal to 0.42, exceeding the value of 0.30 found for the "π" distribution in ethene. An extension of a ring bond path causes the ring cp to migrate toward the cp of the extended bond path increasing its ellipticity that approaches an infinite value. The curvatures of the two cps that lie along their axis of approach both tend to zero and equal zero upon coalescence. The resulting singularity in the density—a cp with a zero curvature along their axis of approach—is structurally unstable and vanishes with further nuclear extension, and the bond path ceases to exist. The density retains the remnants of the vanishing curvature following the bond rupture, and the bond path is reformed through a reversal of these topological changes when the nuclear motions return the system to the domain of the singularity.

The structural change resulting from either the breaking or forming of the ring bond path becomes particularly facile when the ring is conjugated with an unsaturated system in the manner envisaged by Winstein, since there is then a driving force derived from the delocalization of the density over the resulting homoaromatic system. The separation between the ring and "homoaromatic" bond cps is never large, equaling 0.24 au in the 1.612 Å structure displayed in Figure 2. Thus, homoaromatic structures will undergo facile structural changes with the relevant nuclear motions and the presence or absence of a homoaromatic bond path in a particular geometry is not a prerequisite for homoaromatic behavior. It is instead the presence of an internuclear region of "flat" density and its associated electron delocalization that cause the system to be susceptible to the formation or destruction of a singularity in the density. QTAIM analyses should replace the use of dotted lines in representing bonding. Winstein's 1959 proposal[38] of classifying certain molecules as exhibiting homoconjugative or homoaromatic bonding based on the observation of greatly enhanced rates of certain solvolysis reactions is, in effect, defining a class of molecules exhibiting a particular set of characteristic properties in their electron density distributions.

A recent example of a molecule with an equilibrium geometry situated in the structural region of a singularity in the density was noted by Farrugia et al.[47] in the complex of $Fe(CO)_3$ with trimethylene methane. They commented on the absence of bond paths between the iron atom and methine carbon atoms in spite of a delocalization index of 0.57 between the Fe and methine carbon atoms. The missing bond paths from Fe to the three methine carbons can be alternately formed and broken; QTAIM can allow one to define not only structure but the dynamics of structural change through a displacement analysis[14] used here in the case of **1**.

Cope Rearrangement of 1,5-Hexadiene. The recent exhaustive theoretical study of the Cope rearrangement of 1,5-hexadiene by McGuire and Piecuch[10] concluded that **2** rearranges via concerted mechanism involving an "aromatic" transition state, as opposed to a two-stage diradical intermediate. As we mentioned, the calculated energies and geometries obtained here for the chair TS are in good agreement with those reported by McGuire and Piecuch. The activation energy is calculated to be 32.7 kcal mol^{-1}, the experimental value being 33.5 kcal mol^{-1}. Although the chair conformation has an ∼10 kcal mol^{-1} lower activation energy than a starting boat conformation, the boat TS is also investigated because of its structural relation to the boatlike TS found for semibullvalene, as can be seen by comparing **2-TS-b** and **3-TS**. The molecular graphs for the chairlike and boatlike TSs **2-TS-C_{2h}** and **2-TS-C_{2v}** are displayed in Figure 3, parts a and b, respectively. Each is seen to be a symmetrical 6-MR ring structure with the making of the new bond path between C1 and C6 occurring in concert with the breaking of the existing one between C3 and C4. Parts c and d of Figure 3 display the B3PW91 C1|C6 and C6 basins of the boatlike **2-TS-C_{2v}** showing how these basins share a common surface, in keeping with the fact that bond paths exist between C1−C6 and C3−C4.

Topological and Energetic Analyses of the Chair and Boat Transition States. The relatively large activation energies for the Cope rearrangement in **2** do not belie a significant energy stabilization of the transition state as a result of electron delocalization, as is formally possible from the presence of two unsaturated C−C bonds and participation of the pair of electrons linking the two unsaturated three-carbon fragments. The bond orders, delocalization indices, and ellipticities are essentially identical for the chair (**C**) and boat (**B**) starting conformations and are in accord with chemical expectations: C1|C2 $n = 1.96$, DI = 1.84, and $\varepsilon = 0.32$; C2|C3 $n = 1.11$, DI = 1.03, $\varepsilon = 0.03$; C3−C4 $n = 0.95$, DI = 0.99, $\varepsilon = 0.0$. Both the n and DI values indicate that the "π" density of the double bonds is largely localized within the two terminal bonds. One notes the semiquantitative agreement between the empirical (n) and theoretical (DI) measures of bond order.

The chair and boat molecules exhibit similar changes in their bond indices in attaining the ring structures of the TSs. The bond orders of the central bond paths that are, respectively, formed and broken in the σ-bond shift in forming the TS are 0.43 (**C**) and 0.34 (**B**). Overall, the bond orders in the chair TS decrease by 0.4 from their sum in the reactant molecule, the boat TS exhibiting a decrease of 0.6. The delocalization indexes also indicate a decrease in the degree of delocalization of the electrons in attaining the transition states, decreasing by 0.3 for **C** and 0.6 for **B**. The delocalization index for a bond path made or broken in the TS equals 0.60 for **C** and 0.43 for **B**, values consistent with the partial making/breaking of a σ bond. However, these bond paths are essentially σ-like, exhibiting only a vanishingly small ellipticity of 0.02 in the chair TS, and the π-like density is delocalized over the carbons in each of the three-carbon allylic-like fragments, C1|C2|C3 and C4|C5|C6, but it is not contiguous over the intervening σ bonds as anticipated for a molecule emulating an aromatic system. This confinement of the delocalization of the "π" electrons to the three-carbon fragments is further substantiated by the similarity in their bond indices with those for an isolated allylic radical. The radical

bond indices are $n = 1.6$, DI = 1.4, and $\varepsilon = 0.2$ compared with the corresponding TS values of 1.5, 1.3, and 0.2 (**C**) and 1.6, 1.4, and 0.2 (**B**). The DI for the delocalization between the terminal carbons is 0.08 in the isolated radical and in the three-atom fragments. *The TS for the Cope rearrangement of **2** can be described as two allylic-like fragments linked by weak σ bonds.*

This behavior is to be contrasted with the strong elliptical nature of the bond in the hypothetical 1.612 Å homotropylium species, demonstrating that the density delocalized across an "aromatic" gap has a pronounced π component with an ellipticity of 4.3 even though the bond order is less that unity.

The increase in the energies of the carbon atoms account for the activation energies for both starting conformations, increasing by 39 and 43 kcal mol^{-1} for the chair and boat TSs, respectively. The key observation is that the large barriers for both reactions come from the ethylenic carbons C1 and C6, each atom's energy increasing by 22 kcal mol^{-1} (Supporting Information Table 7S). *It is the destabilization of C1 and C6 by a total of 44 kcal mol^{-1} that is the source of the relatively high barrier for the Cope rearrangement of **2***. These increases are a consequence of the loss of "s character" in the hybridization of C1 and C6 in attaining the TSs, as reflected in their loss of electronic charge, 0.04e (**C**) and 0.02e (**B**) accompanying the delocalization of the "π" density over the adjoining bond C2|C3 or C5|C4 to form the three-atom allylic-like fragments C1|C2|C3 and C4|C5|C6. This hybridization argument is verified by the decrease in the stabilization of C1 and C6 when gauged by linear energy relationship that is discussed below. The energies of the interior ethylenic carbons, C2 and C5, change little on attaining the TSs, increasing by 1 and 0.1 kcal mol^{-1} for **C** and **B**, respectively. The energies of C3 and C4 decrease slightly, by 3 (**C**) and 2 (**B**) kcal mol^{-1}, as a result of the transfer of 0.05 (**C**) and 0.08 (**B**) e to their basins. This charge transfer is a consequence of the delocalization of the density from the double bonds to C3 and C4 in forming the three-atom allylic-like fragments C1|C2|C3 and C4|C5|C6.

There is an overall decrease in the stabilization energies in attaining the TSs when these are gauged relative to the linear energy/charge relationship. C2 and C5 are stabilized by ∼20 kcal mol^{-1} in both reactants, retaining their stabilization in the chair TS and increasing by 7 kcal mol^{-1} in the boat TS. The remaining carbon atoms exhibit only small stabilizations in the reactant molecules, but each is destabilized by 13 kcal mol^{-1} in forming the TSs, all four atoms being equally involved in the making and breaking of the "σ bonds".

The energy stabilization/destabilizations found for the atoms in the TSs are similar to those for an isolated allylic radical molecule—studied at UB3PW91/6-311+G(2d,p) but not reported—wherein the terminal carbon atoms, like C1 and C6 or C3 and C4 of the TSs, are destabilized by 9 kcal mol^{-1} and the central carbon, like C2 and C5 of the TSs, is stabilized by 16 kcal mol^{-1}. Thus, the three-membered fragments of the Cope TSs are similar in the stabilization/destabilizations of their atomic energies, as well as in their bond indices, to an isolated allylic radical, a finding consistent with the lack of the delocalization of π-like density over the ring structures of the TSs. The formation of each TS structure results in an overall decrease of 15 kcal mol^{-1} in the stabilization index, and there is no "aromatic stabilization" in their formation. The Cope rearrangement of 1,5-hexadiene proceeds without "aromatic" stabilization of the TS.

Cope Rearrangement of Semibullvalene. The molecular graphs of the reactant, **3-*C*$_S$** (Figure 4a) and the transition state,

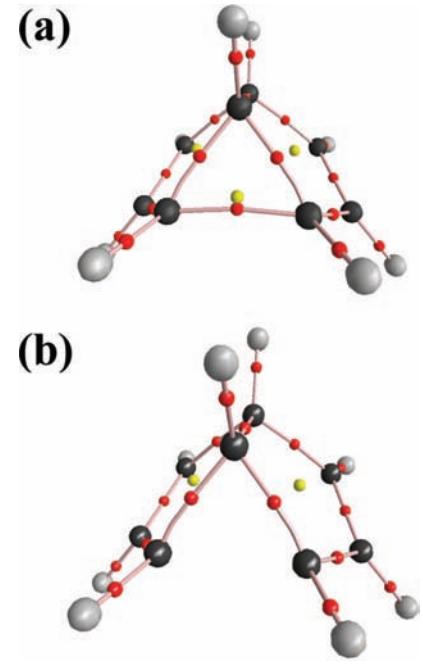

Figure 6. (a) Molecular graph of IRC point with C2−C8 distance of 1.674 Å; (b) molecular graph of IRC point with C2−C8 distance of 1.689 Å.

3-TS-*C*$_{2v}$ (Figure 5a) indicate that the long bond path closing the 3-MR is broken in attaining the structure of the TS. Figure 4b displays the C1 atomic basin of **3-*C*$_S$**. Unlike the Cope rearrangement of **2**, the relatively low barrier of ∼5 kcal mol^{-1} for the rearrangement of semibullvalene leads one to anticipate that a significant delocalization of the density accompanies the attainment of the TS structure. The bond orders for the reactant are in accord with those anticipated on the basis of the classical structure with the relatively long C2|C8 bond path (1.60 Å) exhibiting a bond order less than unity, $n = 0.74$. This weakening of the basal bond path is anticipated because of the proximity of its cp with the cp of the ring, the separation being 0.32 Å, thereby imparting an ellipticty equal to 1.06. This results in a flattening of the density along the line of approach of the bond and ring cps, as reflected in the near equality in their densities that differ by only 0.01 au. The associated curvatures of the density at the ring and bond cps are small and of equal magnitude, ±0.16, a prerequisite for their eventual merging to form a singularity in the density. Clearly, once the singlularity is formed and the C2|C8 bond path vanishes, the residual interaction can be represented by a dotted line, as suggested in the case of the homotropylium ion, to indicate the existence of a significant electron delocalization between the atoms so linked and to the possible reappearance of the bond path with a reversal of the nuclear motion causing its disappearance. The relevant description of the residual interaction upon cleavage of C2|C8 is provided by that between C4 and C6. A DI(C4, C6) = 0.12 indicates that electrons are delocalized to a significant extent between the C4 and C6 basins even in the absence of a bond path. Thus, because of the presence of the 3-MR and the possible formation of a second symmetrically related one, semibullvalene is expected to be a fluxional molecule.

One may track the anticipated change in structure by performing an IRC calculation. One finds that an expenditure of only 0.74 kcal mol^{-1} based on the uncorrected total energies is required to extend the C2|C8 separation by 0.072 Å to 1.674 Å from its equilibrium value of 1.602 Å. The extension decreases the separation between the bond cp and ring cp to

<0.05 Å, increases the ellipticity at the bond cp from 2.06 to 11.88, and brings the values of the two cps to within 0.0001 au of one another with the relevant curvatures, equal to ±0.023 au, approaching zero. The molecular graph of the 1.674 Å geometry is displayed as Figure 6a. A further extension of the C2−C8 distance to 1.689 Å that occurs with an expenditure of 0.26 kcal mol^{-1} leads to the coalescence of the bond and ring cps and to the breaking of the C2|C8 bond path. The molecular graph of this geometry is displayed as Figure 6b.

For **3-C_S**, the DI(C4|C6) = 0.12 is significantly larger than a value of 0.05 that may be taken as a suitable threshold for a homoconjugative interaction. The display of the C5 basin (Figure 4d) indicates the presence a "wedge" of density that intervenes between C4 and C6 precludes bond path formation. A display of the C3 and C7 basins (Figure 4e) with DI(C3|C7) = 0.04 provides support for using 0.05 as DI threshold value for a homoconjugative interaction. Semibullvalene clearly satisfies the criteria for classification as a homoaromatic species, a classification that is further justified with the delocalization of the density found to accompany the formation of the TS.

The classical depiction of the homoaromatic structure for the TS of semibullvalene as shown in **3-TS** indicates a pattern of delocalization that links two allyl groups across the missing bond paths C2|C8 and C4|C6. This structure is recovered in its entirety in the by the theoretical DIs. Although there are no bond paths (Figure 5a), the C2|C8 and C4|C6 DIs equal to 0.38 indicate the presence of a significant "homoaromatic" interaction. Figure 5b shows the C2(C4) and C8(C6) basins. Figure 5c shows the C1(C5) basin that exhibits a "wedge" of density between C2(C4) and C8(C6) thereby precluding bond path formation between these atoms. The two allylic-like fragments exhibit bond indices that are indistinguishable form those for an isolated allylic radical for which $n = 1.6$, $\varepsilon = 0.2$, and DIs = 1.4. Thus, the dotted lines shown in **3-TS** are replicated in the theoretical DI values. This, however, cannot be the complete description of the delocalization of the electrons that accompanies the formation of the TS in **3**, since it is formally the same as that found for the much higher energy rearrangement of the boat conformation of **2**. In this latter case, the allyl groups are linked by bond paths that possess the same DIs of 0.4 as found for the TS of **3**. In **2**, however, the delocalization is confined to the allyl groups, and it is in this respect that the two TSs differ significantly.

The two allyl groups in **3** are linked to one another by the C1|C5 bridge that in the reactant molecule provides the apex atoms for a 3-MR composed of the atoms C1C8C2 or C5C6C4. As discussed above, in the spirit of Winstein, the missing bond paths between the base atoms in the TS have been replaced with a dotted line indicating the presence of a strong homoaromatic interaction. The homotropylium ion demonstrates that the delocalization of the density associated with the surface of a 3-MR is retained even when one of the bond paths is replaced by a homoconjuative interaction. Thus, one finds that the resulting pseudo 3-MRs in **3-TS**, labeled PS-3-MR, exhibit the particular surface delocalization associated with a 3-MR structure and account for the extra stabilization of the TS of **3** over that for the boat TS of **2**.

The structure of **3-TS-C_{2v}** is an 8-MR bisected by C1|C5 to form two 5-MRs, an unsaturated bicyclo[3.3.0]octane with an apex angle of 87°. The surfaces of the PS-3-MBRs are perpendicular to the surfaces of the 5-MRs, as required for efficient delocalization that includes the π density of the 5-MRs. Thus, the major axes of the ellipticities of the bond paths forming the sides of the PS-3-MRs are within 9° of alignment with the ring axis of a 5-MR. The alignment of the same axes in the reactant of **3** are off by 18°. Each of the PS-3-MBR bond paths, with $n = 1.1$, $\varepsilon = 0.1$, and DI = 1.0, is linked to the terminal atom of an allyl group, C2|C3|C4 or C6|C7|C8, whose bond indices are, as described above, indistinguishable from those for an isolated allyl radical: $n = 1.6$, $\varepsilon = 0.2$, and DI = 1.4. The major axes of the allyl bond paths are aligned to within 1° of the ring axis. Although the PS-3-MR bond paths have delocalization indices equal to unity, a nonvanishing bond ellipticity indicates the presence of a π component to the density. Thus, there is a delocalization of π density extending around each 5-MR from C1 to C5 that is conjugatively linked to the density delocalized over the surfaces of the two cp rings. Properties of the density were determined at the midpoint between atoms C2 and C8, the homoaromatic interaction, and midway between the bond cps forming the bonded sides of a PS-3-MR to sample the interior of its surface. The three curvatures of ρ at the midpoint of the homoaromatic interaction between C2 and C8, or alternatively, between C4 and C6, are all of small magnitude yielding $\forall^2\rho = -0.04$ au, with the curvature of smallest magnitude equal to +0.056 au directed along an axis lying in the plane of the PS-3-MR. The value of the density at the midpoint between the bond cps equals 0.24 au, exceeding that at the two bond cps in the ring perimeter by only 0.01 au. The curvatures are thus small in magnitude with $\forall^2\rho = 0.070$ au, with the axis of the smallest curvature, equal to +0.040 au, lying in the plane of the PS-3-MR. These properties emulate those found for the corresponding bond and ring cps in the reactant, and the density is delocalized over the surface of the PS-3-MR. This pattern of electron delocalization represents a significant increase over that found in the reactant molecule, wherein the bond paths C3|C4 and C6|C7 retain their ethylenic character as opposed to its delocalization over the two allylic groups in the TS. Added to this is the delocalization of the density over the surfaces of the two PS-3-MRs.

Winstein[12] pointed out that one can conceive of bishomo- and trishomo- as well as monohomocyclopropenyl, bishomo being of particular interest in the present case wherein each of the bond paths of a PS-3-MR is conjugatively linked to a separate unsaturated 5-MR. Since this bishomo interaction occurs for each PS-3-MR, the TS structure may be viewed as a double bishomoaromatic system.

As anticipated in response to the increase in the homoaromatic interactions in the formation of the TS, all of the carbon atoms are stabilized with respect to the linear charge/energy relationship. This is in contrast to the reactant, where atoms C2, C8, and C5 are destabilized. The delocalization accompanying the formation of the allyl groups within the 5-MRs results in a stabilization of their central atoms, carbons C3 and C7, by 24 kcal mol^{-1}, the largest of the atomic stabilizations. The central atom is also stabilized in the isolated allyl radical, but unlike the isolated group, the terminal atoms of the allyl groups are also stabilized in the TS, by 4 kcal mol^{-1}. The second most stabilized atoms are the bridgehead carbons C1 and C5, stabilized by 12 kcal mol^{-1}, the remaining carbons being stabilized by 4 kcal mol^{-1}.

The atomic origin of the reaction barrier is provided by an analysis of the changes in the atomic energies encountered in the formation of the TS (Table 8S, Supporting Information). The energies of the atoms can be referenced to the energies of the ethylenic carbons C4 and C6. Their bonded neighbors C3 and C7 are slightly less stable. Nearly coincident in energy with the most stable ethylenic carbons is that of the bridgehead atom C1 whose stability is accounted for in terms of the

ethylenic nature of a carbon atom in cyclopropane, the apex bond angle in R equaling 64°. The least stable atom is C5 bonded to two ethylenic carbons and to ethylenic-like C5. It thus has the smallest population with a net positive charge of 0.024e, the only positively charged carbon atom in R. The base atoms of the 3-MR, C2, and C8, are each bonded to an ethylenic carbon and to the bridgehead carbon and thus have intermediate energies.

The largest changes in atomic energies occur for C1 and C5 that become equivalent in TS. The energy of C1 is increased (atom is destabilized) and that of C5 is decreased (atom is stabilized) by almost equal amounts, the atoms losing and gaining electrons, respectively, to yield small net positive charges of +0.009e. The large increase in energy of C1 is a result of the lessening of its ethylenic character—a loss of "s" character—accompanying the opening of the cyclopropane ring. Thus, the low activation energy for the Cope rearrangement of **3** cannot be ascribed to the relief of "ring strain",[4] as the opening of the ring causes an increase in the energy of the apex atom, C1. The redistribution of the electrons from the broken cyclopropane bond path leads to a delocalization of density over the remaining atoms in the newly formed 5-MRs. Each ring consists of an allyl group linked to C1−C5, their common edge. The most stable atoms are the central atoms of the allyl groups, C3 and C7, as found for an isolated allyl group, and they are the most stable carbons in the TS. They are conjugatively linked to their neighboring atoms, C3 to C2 and C4, and C7 to C8 and C6. C2 and C8 decrease in energy by an amount almost equal to the increase in energy of C4 and C6. It is the density of these latter atoms that is delocalized onto C2 and C8 in the formation of the allyl groups. Although the changes in the energies of the carbon atoms nearly cancel, their sum equaling −2.6 kcal mol^{-1}, *it is the unexpected dramatic increase in the stability of the bridgehead atom C5 that makes the largest single contribution to lowering the barrier for the degenerate rearrangement of **3***. This decrease in the energy of C5 in attaining the TS structure is the result of a number of factors all of which act in concert: a decrease in the C5 bridgehead angle from 100° in R to 87° in TS, causing an increase in its "s" character thus increasing its energetic stability and electronegativity, as reflected in the increase of 0.02e in its population, an increase in the delocalization of the electrons that extends to the bridgehead atoms, accounting for the increase of 23 kcal mol^{-1} in the linear charge/energy stabilization of C5. The changes in the energies of the hydrogen atoms are all of smaller magnitude than those for the carbons. They sum to 8.4 kcal mol^{-1} with the largest contributions coming from the H atoms bonded to the carbons in the cp ring.

In summary, the driving force for the Cope rearrangement of semibullvalene is not the relief of ring strain but is rather a consequence of the delocalization—excluding the bridgehead bond path C1−C5—of π-like density around the atoms of both 5-MRs and the dramatic stabilization of C5. These two systems are in turn linked by the delocalization of the density over the surfaces of the PS-3-MRs, whose bond paths are common to both 5-MRs. The TS for the rearrangement of semibullvalene is stabilized by a double bishomoaromatic delocalization of the density.

Displacement Analysis of 3. On the basis of a G03 frequency calculation on **3**, there are two normal modes (474 cm^{-1} and 674 cm^{-1}) that stretch the C2|C8 bond of the 3-MR. Using ChemCraft we found that by using a scaling factor of 0.35 for the 474 cm^{-1} mode yielded a maximum C2|C8 internuclear distance of 1.708 Å. Freezing the nuclear motions at this point yielded a geometry that exhibited no bond cp between C2|C8 and that was 4.02 kcal mol^{-1}—this value is close to the experimental barrier for the degenerate rearrangement of **3**—higher in energy that the equilibrium geometry of **3**. Given that the 474 mode has a ZPE of 0.68 kcal mol^{-1}, **3** is not fluxional at 0 K.

Conclusions

This study of the Cope rearrangement in semibullvalene has demonstrated that QTAIM provides a physical basis for Winstein's definition of homoaromaticity. His 1959 proposal of classifying certain molecules as homoconjugative or homoaromatic, one based on the observation of greatly enhanced rates of certain solvolysis reactions, is shown to effect the definition of a class of molecules exhibiting a particular set of properties in their electron density distributions. It is remarkable how well a model of a particular form of electron delocalization based on experimental solvolysis rates maps onto a set of properties exhibited by a molecular charge distribution. The mapping entails the transcription of the concepts of electron delocalization and aromaticity and, in addition, accounts for the structural lability of homoaromatic molecules. As well as recovering familiar concepts such as bond order, electron delocalization, and "π character", QTAIM makes possible a way of quantifying the relation between hybridization and an atom's energy and electronegativity. Most important, the paper demonstrates that homoaromatic molecules exhibit residual "homoaromatic interactions" even in the absence of the bond path anticipated on the basis of the dotted lines employed to portray their presence in a semiclassical structure. Such interactions are identified by significant nonbonded interatomic delocalization indices and "flat" interatomic density distributions whose presence portends the formation of a bond path and a change in structure. It is hoped that the paper may serve as a bridge between orbital models and the underlying physics

Acknowledgment. E.C.B. thanks Loyola University Chicago for a generous allotment of startup funds. N.H.W. gratefully acknowledges financial support by the Natural Science and Engineering Research Council of Canada. We thank SHARCNET (Shared Hierarchical Academic Research Computing Network (of Ontario) for providing computing resources at McMaster University.

Supporting Information Available: Complete ref 19, tables of total energies and thermochemical data at PBE1PBE/6-311+G(2d,p) and tables of values of the density at bond critical points and delocalization indexes at B3PW91 and PBE1PBE, tables of atom energies, molecular graphs of 1,5-hexadienes, and plot of carbon atom energy versus atom electron populations for ethane, ethane, and ethyne. This material is available free of charge via the Internet at http://pubs.acs.org.

References and Notes

(1) Childs, R. F. *Acc. Chem. Res.* **1984**, *17*, 347.
(2) Hoffmann, R.; Stohrer, W.-D. *J. Am. Chem. Soc.* **1971**, *93*, 6941.
(3) Williams, R. V. *Chem. Rev.* **2001**, *101*, 1185.
(4) Jackman, L. M.; Fernandes, E.; Heubes, M.; Quast, H. *Eur. J. Org. Chem.* **1998**, 2209.
(5) Williams, R. V. *Eur. J. Org. Chem.* **2001**, 227.
(6) Hrovat, D. A.; Williams, R. V.; Goren, A. C.; Borden, W. T. *J. Comput. Chem.* **2001**, *22*, 1565.
(7) Brown, E. C.; Henze, D. K.; Borden, W. T. *J. Am. Chem. Soc.* **2002**, *124*, 14977.
(8) Hrovat, D. A.; Brown, E. C.; Williams, R. V; Quast, H.; Borden, W. T. *J. Org. Chem.* **2005**, *70*, 2627.

(9) Borden, W. T. Ab Initio and DFT Calculations on the Cope Rearrangement, a Reaction with a Chameleonic Transition State. In *Theory and Applications of Computational Chemistry: The First Forty Years*; Dystra, C. E., Frenking, G., Kim, K. S., Scuseria, G. E., Eds.; Elsevier B. V.: Amsterdam, The Netherlands, 2005; pp 859−873.

(10) McGuire, M. J.; Piecuch, P. *J. Am. Chem. Soc.* **2005**, *127*, 2608.

(11) Bader, R. F. W. *Atoms in Molecules*; Oxford Science Publications: Oxford, U.K., 1990.

(12) Winstein, S. *Q. Rev., Chem. Soc.* **1969**, *23*, 141.

(13) Bader, R. F.W. *J. Chem. Phys. A* **2007**, *111*, 7966.

(14) Bajorek, T.; Werstiuk, N. H. *Can. J. Chem.* **2005**, *83*, 1352.

(15) Poulsen, D. A.; Werstiuk, N. H. *J. Chem. Theory Comput.* **2006**, *2*, 77.

(16) Werstiuk, N. H. *J. Chem. Theory Comput.* **2007**, *3*, 2258.

(17) Werstiuk, N. H.; Sokol, W. *Can. J. Chem.* **2008**, *86*, 737.

(18) Werstiuk, N. H.; Poulsen, D. A. *ARKIVOC* **2009**, *Part v*, 38.

(19) Frisch, M. J.; et al. Gaussian 03, revisions B.02 and C.02; Gaussian, Inc.: Wallingford, CT, 2004.

(20) Werstiuk, H. H.; Muchall, H. M.; Noury, S. *J. Phys. Chem. A* **2000**, *104*, 11601.

(21) Kirchner, B.; Sebastiani, D. J. *J. Phys. Chem. A* **2004**, *108*, 11728.

(22) Dennington, R., II; Keith, T.; Millam, J.; Eppinnett, K.; Hovell, W. L.; Gilliland, R.; GaussView, version 3.09; Semichem, Inc.: Shawnee Mission, KS, 2003.

(23) Biegler-Konig, F. AIM 2000; University of Applied Science: Bielefeld, Germany, 1998−2000.

(24) Fradera, X.; Austen, M. A.; Bader, R. F. W. *J. Phys. Chem. A* **1999**, *103*, 304.

(25) Wang, Y.; Matta, C.; Werstiuk, N. H. *J. Comput. Chem.* **2003**, *24*, 1720.

(26) Wang, Y.; Werstiuk, N. H. *J. Comput. Chem.* **2003**, *24*, 37.

(27) Wang, Y.-G.; Wiberg, K. B.; Werstiuk, N. H. *J. Phys. Chem. A* **2007**, *111*, 3592.

(28) Keith, T. A. AIMALL97 Package (A3) for Windows. aim@tkgristmill.com.

(29) ChemCraft, version 1.5. http://www.chemcraftprog.com.

(30) Wang, Y. C.; Bauer, S. H. *J. Am. Chem. Soc.* **1972**, *94*, 5651.

(31) Christoph, G. G.; Beno, M. A. *J. Am. Chem. Soc.* **1978**, *100*, 3156.

(32) Doering, W. v. E.; Toscano, V. G.; Beasly, G. H. *Tetrahedron* **1971**, *27*, 5299.

(33) Goldstein, M. J.; Benzon, M. S. *J. Am. Chem. Soc.* **1972**, *94*, 7147.

(34) Cheng, A. K.; Anet, F. A.; Mioduski, J.; Meinwald, J. *J. Am. Chem. Soc.* **1974**, *96*, 2887.

(35) Moskau, D.; Aydin, R.; Leber, W.; Günther, H.; Quast, H.; Martin, H.-D.; Hassenrück, K.; Miller, L. S.; Grohmann, K. *Chem. Ber.* **1989**, *122*, 925.

(36) Cremer, D.; Kraka, E.; Slee, T. S.; Bader, R. F. W.; Lau, C. D. H.; Nguyen-Dang, T. T.; MacDougall, P. J. *J. Am. Chem. Soc.* **1983**, *105*, 5069.

(37) Cremer, D.; Childs, R. F.; Kraka. E. Cyclopropyl Homoconjugation, Homoaromaticity and Homoaromaticity—Theoretical Aspects and Analysis. In *The Chemistry of the Cyclopropane Group*; Rappaport, Z., Ed.; John Wiley & Sons Ltd.: New York, 1995; Vol. 2, pp 339−409.

(38) Winstein, S. *J. Am. Chem. Soc.* **1959**, *81*, 6524.

(39) Walsh, A. D. *Nature (London).* **1947**, *159*, 712.

(40) Walsh, A. D. *Trans. Faraday Soc.* **1949**, *45*, 179.

(41) Bader, R. F. W.; Laidig, K. E. *THEOCHEM* **1992**, *261*, 1.

(42) Bader, R. F. W. Atoms in Molecules. In *Encyclopedia of Computational Chemistry*; Schleyer, P. v., Ed.; John Wiley and Sons: Chichester, U.K., 1998; Vol. 1, pp 64−86.

(43) Coulson, C. A. *Valence*, 2nd ed.; Oxford University Press: Oxford, U.K., 1961; p 250.

(44) Coulson, C. A.; Moffitt, W. E. *Philos. Mag.* **1949**, *40*, 1.

(45) Benson, S. W.; Cruickshank, F. R.; Golden, D. M.; Haugen, G. R.; O'Neal, H. E.; Rodgers, A. S.; Shaw, R.; Walsh, R. *Chem. Rev.* **1969**, *69*, 279.

(46) Cremer, D.; Reichel, F.; Kraka, E. *J. Am. Chem. Soc.* **1991**, *113*, 9459.

(47) Farrugia, L. J.; Evans, C.; Tegel, M. *J. Phys. Chem. A* **2006**, *110*, 7952.

JP8109385